

A Python Implementation of the Multisection Model for Simulation of MDG-impaired SDM Channels

Humberto V. Q. Melo, Ruby S. B. Ospina and Darli A. A. Mello

Abstract—Space division multiplexing (SDM) is a promising solution to increase the capacity of current optical networks. However, the capacity increase provided by SDM is limited by mode-dependent gain (MDG) generated in amplifiers. To enable the study of MDG-impaired SDM transmission, analytical models can be employed to simulate SDM channels at different MDG levels. In this paper, we implement the analytical multisection model for strongly-coupled SDM transmission in Python language. Based on the implemented model, we validate the theoretical capacity distribution for two polarization modes and study the frequency diversity effect in SDM channels.

Keywords—Space division multiplexing, multisection model.

I. INTRODUCTION

Space division multiplexing (SDM) technology in optical fiber communication systems is being studied as an alternative solution to overcome the exponential growth of data traffic resulting from the emergence of big data, intense social networking, real-time gaming, and cloud services. Coupled SDM transmission has been successfully demonstrated in experiments over coupled-core multi-core fiber (MCFs) [1], multi-mode fibers (MMFs) [2], few-mode fibers (FMFs) [3], and few-mode multicore fibers (FM-MCFs) [4].

In transmission with mode division multiplexing (MDM), propagation modes are used as parallel channels. These parallel channels exhibit different group delays (GDs) that result in modal dispersion (MD) [5]. Furthermore, for ultra-long haul optical systems, many in-line components, particularly Erbium-doped fiber amplifiers (EDFAs), are required. These components can introduce mode-dependent loss (MDL) and mode-dependent gain (MDG), here referred jointly to as MDG. MDG is a performance-limiting factor for SDM systems and can lead to a significant decrease in channel capacity [6]. As MDG limits the capacity of SDM systems, its effect should be accurately studied in simulation contexts or through analytical models for system performance evaluation and problem addressing. This paper presents a Python-based implementation of an SDM channel based on the multisection model proposed in [6], focusing on the study of the capacity and MDG. Two important results are outlined:

- A validation of the multisection model by comparing the capacity probability density function (PDF) found through this numerical model and by the analytical curve proposed by Mello et al. in [7].
- A validation of the frequency diversity effect, firstly observed by Ho and Kahn in [8].

Humberto V. Q. Melo, Ruby S. B. Ospina and Darli A. A. Mello, School of Electric and Computer Engineering, Unicamp, Campinas, SP, Brazil, e-mail: h172417@dac.unicamp.br, r163653@dac.unicamp.br, darli@unicamp.br. This work was partially supported by Fapesp grants 2022/07488-8, 2015/24341-7 and 2022/05753-6

II. MULTISECTION MODEL AND CAPACITY OF MDG-IMPAIRED SDM CHANNELS

Random coupling among propagation modes can be caused by fiber bends, thermal gradients, roughness at the core-cladding boundary, variations in the core radius, and other effects. A numerical model to study the statistics of MDG in SDM transmission with strong coupling was proposed in [6]. The multisection model for strongly-coupled SDM transmission models the fiber as a concatenation of K independent sections. In the multisection model, each section of the fiber is represented by a $(D \times D)$ transfer matrix given by

$$\mathbf{H}^{(k)}(\omega) = \mathbf{V}^{(k)} \mathbf{\Lambda}^{(k)}(\omega) \mathbf{U}^{(k)H}, \quad (1)$$

where D is the number of propagation modes accounting for spatial paths and polarization states. \mathbf{V} and \mathbf{U} are unitary random matrices that characterize coupling between modes at the input and at the output of the section, respectively. The superscript $(\cdot)^{(k)}$ denotes the k_{th} section and $(\cdot)^H$ denotes Hermitian operator. The matrix $\mathbf{\Lambda}$ accounts for MDG and GD and is computed as [7]

$$\mathbf{\Lambda}^{(k)}(\omega) = \text{diag} \left[\exp \left(\mathbf{g}^{(k)} / 2 - j\omega \boldsymbol{\tau}^{(k)} \right) \right], \quad (2)$$

where $\mathbf{g}^{(k)}$ is the uncoupled modal gain vector and $\boldsymbol{\tau}^{(k)}$ is the uncoupled GD vector. Also, $\exp(\cdot)$ denotes element-wise exponential, and $\text{diag}[\cdot]$ denotes a diagonal matrix formed by placing the argument vector on the main diagonal.

To study the accumulated effect of MDG and GD at the end of the link, in the strong coupling regime, the overall transfer matrix is computed by multiplying the K transfer matrices as

$$\mathbf{H}^{(t)}(\omega) = \prod_{k=1}^K \mathbf{H}^{(k)}(\omega) = \mathbf{V}(\omega) \mathbf{\Lambda}(\omega) \mathbf{U}^H(\omega), \quad (3)$$

where $(\cdot)^{(t)}$ denotes the overall contribution of all sections.

From the overall transfer matrix, the elements of the overall gain vector can be calculated as the logarithm of λ_i , which are the eigenvalues of the operator $\mathbf{H}(\omega) \mathbf{H}(\omega)^H$.

For a fair comparison between frequency channels, the transfer matrix, \mathbf{H} , must be divided by a normalization factor as [7]

$$\mathbf{H}(\omega) = \frac{\mathbf{H}^{(t)}(\omega)}{\sqrt{\frac{1}{D} \sum_{i=1}^D \mathbb{E}\{e^{g_i^{(t)}}\}}}}. \quad (4)$$

Once the normalized overall transfer matrix is computed, the capacity of a narrow band channel impaired by MDG,

C_{mdg} , can be calculated through [7]

$$C_{mdg} = \sum_{i=1}^D \log_2 \left(1 + \frac{SNR}{D} \lambda_i \right), \quad (5)$$

where the signal-to-noise ratio (SNR) is defined as the sum of the signal power in all modes divided by the noise power per mode.

III. SIMULATION AND RESULTS

Using Numpy and Matplotlib libraries, a code was developed to numerically simulate SDM channels based on the numerical multisection model described in Section II. The code can be employed to estimate important channel parameters such as MDG and capacity.

For implementing the multisection model, firstly, the number of modes, D , number of fiber sections, K , section length L (in km), GD standard deviation (STD), μ (in ps/km), and the STD of MDG per section, σ_g , are defined.

The uncoupled gain vector $g^{(k)}$ is computed as a D -sized array where half the entries are σ_g and the other half are $-\sigma_g$. Additionally, the $\tau^{(k)}$ vector is computed as a D -sized array with Gaussian distributed entries that sum to zero and have STD $\mu_{gd} = \mu \times \sqrt{L}$ [9]. Accordingly, the σ_g and μ_{gd} parameters are sufficient to describe the MDG and MD in strongly-coupled transmission [6], [10].

For each section, the \mathbf{U} and \mathbf{V} matrices are computed as shown in the appendix of [6]. Since the overall transfer matrix is frequency dependent, $\mathbf{H}^{(t)}(\omega)$ is computed from Eqs. (2) and (3), for an F number of equally spaced frequency bins over a fixed bandwidth B_w . Finally, for narrow band frequency channel ω_0 , $\mathbf{H}^{(t)}(\omega_0)$ is normalized by the square root of the mean of the overall coupled modal power gains at all frequencies as in Eq. (4).

A. Capacity estimation

As a consequence of random coupling, the capacity of an MDG-impaired SDM channel behaves as a random variable. The equations presented in Section II and the steps described at the beginning of this section for implementing the multisection model corresponds to a single realization of the capacity random variable. Therefore, in order to describe the capacity through a probabilistic distribution, the same process is repeated R times to compute a large number of capacity realizations. Then, the PDF of the capacity of an SDM channel with D propagation modes can be numerically computed. The theoretical PDF for $D = 2$ and the PDF numerically obtained by using the multisection model are depicted in Fig. 1. The figure shows that the capacity PDF obtained by employing the Python implementation of the multisection model tracks with high accuracy the theoretical PDF for the capacity.

B. Frequency diversity

The presence of MD and MDG generates a frequency-selective channel. For high levels of MD, the channel frequency response varies rapidly reducing the capacity fluctuations caused by MDG, an effect known as frequency diversity. In [8], it is observed that a normalized bandwidth $b = B_w \mu_{gd} \gg 1$ guarantees independent realizations of channel

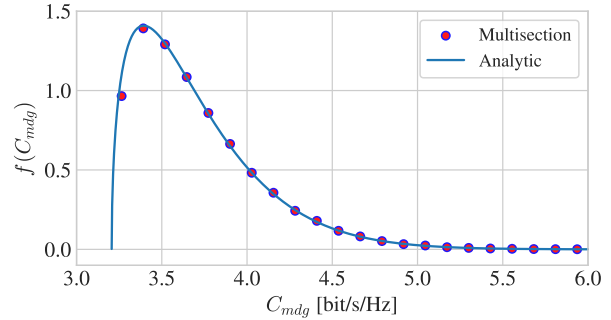


Fig. 1: PDF of the instantaneous capacity C_{mdg} of a narrowband channel in linear scale. The continuous curve is obtained with the analytic expression for the capacity and the markers are computed with $R = 100,000$ realizations of the multisection model. A cascade of $K = 300$ sections is considered, each with length $L = 50$ km. MDG per amplifier is $\sigma_g = 0.3$ dB, and $SNR/D = 6.2$ dB.

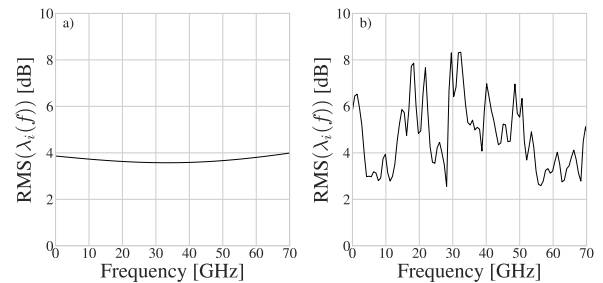


Fig. 2: Root mean square (RMS) of λ_i in dB for low (a) and high (b) MD, respectively.

capacity, so instantaneous capacity approaches the average capacity, as an implication of the law of large numbers. Fig. 2 shows the frequency diversity effect on the MDG. With frequency diversity, each modal gain varies rapidly between shallow and deep fading regions, impacting the overall MDG. In Fig. 2a, for low-frequency diversity, the MDG varies smoothly with frequency, presenting high correlation, even for distant frequencies. In contrast, in Fig. 2b, for high-frequency diversity, the MDG varies rapidly, reducing the correlation of distant frequencies.

IV. CONCLUSIONS

This paper presents a Python-based implementation of the multisection model for strongly-coupled SDM transmission. The performed simulations reproduce important results of SDM-related works, validating the multisection model through the PDF of the capacity for $D = 2$ and the inspection of the frequency diversity effect. For further analysis, this numerical model can be used to find the PDF of the capacity for a higher number of modes with respect to different parameters, such as σ_g and μ_{gd} .

REFERENCES

- [1] R. Ryf *et al.*, Proc. of OFC, paper Th4B.3, (2019).
- [2] J. van Weerdenburg *et al.*, Proc. of ECOC, pp.1-3, (2018).
- [3] G. Rademacher, *et al.*, J. Lightw. Technol., **36**, pp.1382-1388, (2017).
- [4] D. Soma *et al.*, Proc. of ECOC, pp. 1-3, (2017).
- [5] D. J. Richardson, *et al.*, Nature photon., **7**, pp.354-362, (2013).
- [6] K.-P. Ho *et al.*, Optics express, **19**, pp.16612-16635, (2011).
- [7] D. A. Mello, *et al.*, J. Lightw. Technol., **38**, pp.303-318, (2019).
- [8] K.-P. Ho *et al.*, J. Lightw. Technol., **29**, pp.3719-3726, (2011).
- [9] R. S. Ospina, *et al.*, J. Lightw. Technol., **39**, pp.1968-1975, (2020).
- [10] K.-P. Ho *et al.*, J. Lightw. Technol., **29**, pp.3119-3128, (2011).